ON START TO END SIMULATION AND MODELING ISSUES OF THE MEGAWATT PROTON BEAM FACILITY AT PSI

A. Adelmann, S.Adam, H-R.Fitze, R.Geus, M.Humbel, L.Stingelin, PSI, Villigen, Switzerland

Abstract

Start to end simulations are discussed in the light of our plans for a 3 mA, 1.8 MW proton beam at the PSI cyclotron facility [1].

MOTIVATION

Within the scope of the high intensity upgrade described in [2, 1] and maintaining the outstanding performance with respect to *low losses* and *high availability*, there is a strong imperative, for start to end simulations of our proton cyclotron facility. There are two levels of understanding: *qualitative* and *quantitative*. Our aim is to improove on the quantitative level in order to have a theoretical model available which allows us to accurate: i) match diagnostics like (rms) beam sizes and tunes ii) predicting losses and iii) predict new operation modes.

TOOLS

From the modeling side, there are two major areas of endeavor: **space charge** which implies (large) n-body simulations and **large range of scales** which must be resolved. A careful selection and implementation of the used models are of utmost importance and are described in the next sections.

Space Charge Solvers

When modeling space charge dominated beams, one of the key elements is accurate and fast Poisson solvers. The fundamental steps in calculating $\vec{E}$, the electric self field are: a Lorentz transformation in the beam's rest frame $x' = \mathcal{L}(x)$, interpolation of $q_i(x')$ to obtain ρ, the charge density on a discrete space (grid). Then we solve:

$$-\triangle u = \frac{\rho}{\epsilon_0} \quad \text{on } \Omega, \tag{1}$$
$$u = 0 \quad \text{on } \partial\Omega, \tag{2}$$

where $\Omega \subset \mathcal{R}^3$ is a bounded domain, $x \in \Omega$ and ϵ_0 is the permittivity of vacuum. We then obtain the fields in the beam frame: $\vec{E}' = -\nabla u, \quad \vec{B}' = 0$ followed by an interpolation: $\vec{E}'(x')$ at particle positions x' from $\vec{E}'$. The back transformation to the beam frame $\{\vec{E}(x), \vec{B}(x)\} = \mathcal{L}^{-1}(\vec{E}')$ ends the field calculation.

One of the most used solvers is direct FFT based solvers (no discretization of the $\triangle$-operator). G denotes the Greens function in open space, while variables with hats are in Fourier space. To obtain the scalar potential in the beam frame, we interpolate ρ and G onto a rectangular grid, followed by a Fourier transform to obtain $\widehat{\rho}$ and $\widehat{G}$. Determining $\widehat{u} = \widehat{\rho} * \widehat{G}$ and transforming them back gives $u = FFT(\widehat{u})^{-1}$. Computing $\vec{E}' = -\nabla u$ using a second order finite difference scheme and interpolate $\vec{E}'(\vec{x'})$ at particle positions $\vec{x'}$ from $\vec{E}'$. The use of FFT reduced the computational complexity from $\mathcal{O}(N^2)$ to $\mathcal{O}(N \log N)$ with N denoting the grid size. Using parallel FFT's one can easily parallelize this scheme and integrate it into a particle tracking program [3].

In the case of large and complicated boundaries we propose a finite element based Poisson solver (using trilinear finite elements) with a semi unstructured grid [4]. The resulting linear system of equation is then solved with a multigrid. A multigrid algorithm [5] is used to solve the linear system of equations resulting from the finite element discretisation. Table 1 shows excellent scalability with respect to the problem size M which is equivalent to handle in the order of 10^{11} *macro particles* in simulation with reasonable computing time. For this scaling study we use the Seaborg (IBM SP-3) computer at NERSC.

P	M	$T_g P/M$	T	TP/M
8	625,464	3.5e-3	3.1	3.9e-5
32	306,080	8.5e-3	0.78	8.1e-5
248	4,751,744	5.90e-3	1.2	6.2e-5
248	36,998,619	7.50e-3	7.7	5.1e-5
960	23,312,735	4.85e-3	4	1.64e-4
2025	405,242,845	6.60e-3	10.7	5.3e-5
4075	7,166,171,845	8.76e-3	160	9.9e-5

Table 1: Scalability of the parallel grid generator $T_g P/M$ and the Poisson solver showing also T, the time in seconds for one Multigrid step.

MAD9P (*M*ethodical *A*ccelerator *D*esign version *9* - *p*arallel)

MAD9P is a general purpose parallel particle tracking program including three-dimensional space charge calculation [3]. MAD9P is based on the Vlasov-Maxwell equations. In this model, particle motion is governed by external fields and a mean-field approach for the space-charge fields. Particle collisions and radiation are neglected. The total Hamiltonian for a beam line element can be written as a sum of two parts, $\mathcal{H} = \mathcal{H}_1 + \mathcal{H}_2$, which correspond to the external and space charge contributions. A second-order integration algorithm (split operator) for a single step

is then given by

$$\mathcal{M}_k(\tau) = \mathcal{M}_k^1(\tau/2)\,\mathcal{M}_k^2(\tau)\,\mathcal{M}_k^1(\tau/2) + \mathcal{O}(\tau^3) \quad (3)$$

where τ denotes the step size, $\mathcal{M}_k^1$ is the map corresponding to $\mathcal{H}_1$ obtained by differential algebra methods from a general relativistic Hamiltonian and $\mathcal{M}_k^2$ is the map corresponding to $\mathcal{H}_2$. $\mathcal{M}_k^2$ is obtained by discretizing the resulting Poisson problem on a rectangular mesh using Fourier techniques, as described in the second section of this paper. Open and periodic boundary conditions can be chosen. Once the physical elements are put together in an arbitrary way the elements are assumed to be perfectly aligned. To every beam element belongs a corresponding transfer map $\mathcal{M}_k^2$ which maps every initial condition ζ^i of the six dimensional phase space onto a final condition ζ^f by $\zeta^f = \mathcal{M}_k^2 \zeta^i$. MAD9P derives $\mathcal{M}^2$ by a *Lie algebraic method*.

Modeling RF-Structures

To further increase the accuracy of the simulation we replace the thin lens approximation by full particle tracking in the RF cavity. Thus, both the electric field $\vec{E}(\vec{x},t)$ and the magnet field $\vec{B}(\vec{x},t)$ need to be known in the cavity. Therefore the standing electro-magnetic waves in the cavity with the lowest frequencies have to be determined. This amounts (after separation of time/space variables and after elimination of the magnetic field intensity) to solving the eigenvalue problem

$$\begin{aligned}
\nabla \times \nabla \times \vec{e}(\vec{x}) &= \lambda\,\vec{e}(\vec{x}), & \vec{x} \in \Omega, \\
\nabla \cdot \vec{e}(\vec{x}) &= 0, & \vec{x} \in \Omega, \quad (4) \\
\vec{n} \times \vec{e} &= 0, & \vec{x} \in \partial\Omega,
\end{aligned}$$

where $\lambda = \omega^2/c^2$ and $\vec{e}$ is the normalized electric field intensity. We use the weak formulation proposed by Kikuchi [6].

We discretise the field $\vec{e}$ by second order edge elements proposed by Nédélec [6] the Lagrange multiplier are second order node elements. This yields a large sparse constrained matrix eigenvalue problem. The eigenvalue problem is solved numerically using our own implementation of the Jacobi-Davidson (JD) algorithm introduced by Sleijpen-van der Vorst [6]. The calculated E- and B-fields
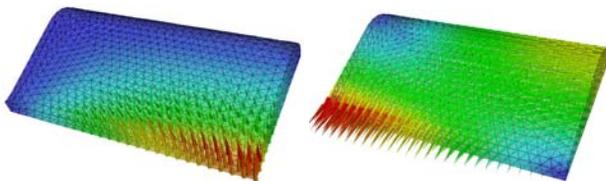
Figure 1: color: E- (left) and B-fields (right) of the fundamental mode in the new cavity of the PSI 590 MeV ring cylotron.

in the cavity (cf. Fig. 1) will be soon integrated into the MAD9P tracking code.

Efficient Parallelization

Efficient parallelization of a code can only be achieved if the code is implemented in a suitable language, for example C++ and MPI (Message Passing Interface) augmented with the concept of expression templates originally proposed in [7]. This ansatz allows C++ to achieve the same performance on vector and matrix expressions as with Fortran. Expression templates are used in MAD9P, explained in the subsequent section. The eigenvalue solver discussed above, is implemented in C++ using Trilinos [8], a collection of robust parallel solver algorithms for large-scale scientific applications.

FROM 870 KEV TO 590 MEV

Next we show simulations and results all the way from the 870 keV injection line to the Ring cyclotron.

B870 Injection Line

The starting point for all B870 injection line calculations is a 4-dimensional transverse phase space distribution, which has been proven satisfactory by its use in the daily operation of the beam line. The longitudinal dimensions are uniform in space and momenta. The initially DC beam is modeled by using a characteristic longitudinal beam length of $\beta\lambda$, where λ is the wave length of the RF. The double gap buncher is modeled by (analytic) sinusoidal momenta modulation of the beam. Fig. 2 shows the horizontal beam envelope (similar results are obtained in the vertical direction after fitting the 4-dimensional transverse distribution and a global space-charge neutralisation factor f_e using a stochastic fit algorithm based on Simu-
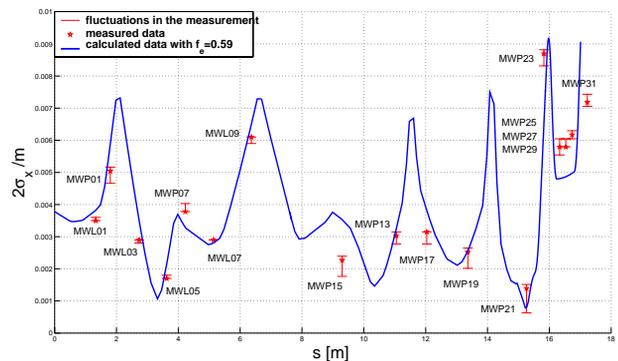
Figure 2: color: Horizontal beam profiles.

lated Annealing.

Good agreement between measurement and simulation is obtained, the space-charge neutralisation factor $f_e = 0.59$ is in the expected range (for reference see [3]).

Injector 2, Coasting Beam

A model of the Injector 2 lattice based on hard-edge elements is used for various coasting beam simulations. The

2D results of Adam [9], which predict a stable round distribution in horizontal- longitudinal configuration space has been verified (see Fig. 3) with the full three-dimensional model. The data shown in Fig. 3 are for $5\ MeV$ and $1\ mA$. The effect of the beam intensity on the development of the
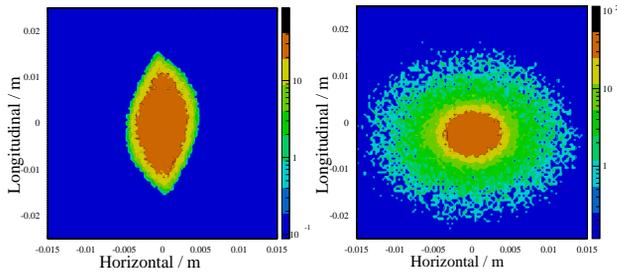
Figure 3: color: Charge density in a.u.: Turn 1 and 60.

rms beam sizes in the horizontal and longitudinal directions is shown in Fig. 4 for 60 turns. The strong oscillations in the first few turns are due to an initial 'mismatch' of the beam. The fact that the rms beam size increases with increasing beam current strongly suggests that a detailed understanding of the matching condition might be the key to a very fast development of the desired round and stable distribution.
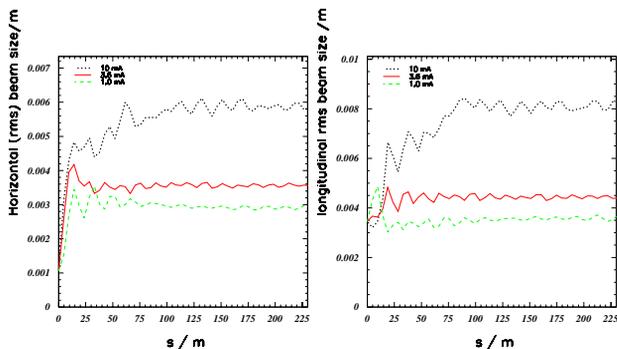
Figure 4: color: Horizontal and Longitudinal rms beam sizes at different intensities over 60 turns.

Injector 2 Including Collimation

To fix the non trivial initial conditions we start with one turn and the estimated particle distribution from [3]. After lengthy precision work on positioning the collimators and fine tuning details of injections, we were able to simulate the very beginning of Injector 2 with satisfactory results. The amount of beam deposition on some collimators as well as the collimation process shown in Fig. 5 are well in agreement with observation. The z-axis is the direction of beam propagation and the x-axis points to the center of the cyclotron. Looking at Fig. 5 makes it clear that the bunch center rotates itself, the lower arm is expanding and the bunch has been collimated at the right place. The acceleration model in MAD9P is thus usable and promises detailed beam dynamic analysis in the near future.
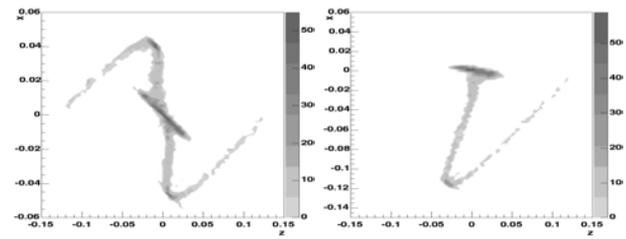
Figure 5: Spatial particle density in a.u before KIP1 and after KIP2.

Ring Beam-Cavity Interaction

A mode-expansion method [10] is used for the representation of beam-excited fields in the ring cyclotron. For the determination of the mode amplitudes and phases it is required to calculate the parameters of zero beam-current trajectories from cyclotron injection to extraction.

The ESIL eigenmode solver in Omega3P allows to calculate Higher Order Modes (HOMs) of the entire cyclotron-structure as basis functions for the mode-expansion. A set of 280 eigenmodes with resonance frequencies close to harmonics of the beam-crossing frequency is found and 30 particularly critical modes are selected. Their eigenfields are interpolated onto a structured, cylindrical grid, located in the midplane.

Subsequent tracking of about 100'000 macro-particles with with 2d space-charge corrections and comparing the beam-shapes of a simulation with consideration of HOMs to results from a HOMless simulation indicates that the effect of beam-excited fields onto the beam-quality is relatively small for the beam-currents of about 2mA.

REFERENCES

[1] P. A. Schmelzbach et.al, "Steps Towards a 3 mA, 1.8 MW Proton Beam at the PSI Cyclotron Facility", PAC 2005.

[2] H.R. Fitze, "Developments at PSI (including new RF cavity)", Cyclotrons 2004.

[3] A. Adelmann, "3D Simulations of Space Charge Effects in Particle Beams", PhD Thesis, ETH Zurich (2002).

[4] C. Pflaum, "Semi-unstructured grids, Computing", (2001) 67.

[5] U. Trottenberg, C.W. Oosterlee, A. Schüller, "Multigrid", Academic Press (2001).

[6] R. Geus, "The Jacobi–Davidson algorithm for solving large sparse symmetric eigenvalue problems", PhD Thesis No. 14734, ETH Zurich (2002).

[7] T. Veldhuizen, "Expression templates", C++ Report 1995 7.

[8] M.A. Heroux and J.M. Willenbring, "Trilinos Users Guide", Sandia National Laboratories (2003).

[9] S.R. Adam, PhD thesis No. 7694 ETH Zurich (1985).

[10] L. Stingelin et al., "Beam Cavity Interaction Simulation for the PSI Ring-Cyclotron", Cyclotrons 2004.